Food Chemistry: X 12 (2021) 100157

Contents lists available at ScienceDirect

Food Chemistry: X

journal homepage: www.sciencedirect.com/journal/food-chemistry-x

Structural characterization and protective effects of polysaccharide from *Gracilaria lemaneiformis* on LPS-induced injury in IEC-6 cells

Xiong Li [a,b,1], Yufeng Gong [a,b,1], Wanzi Yao [a,b], Xiaoyong Chen [a,b], Jiebei Xian [c], Lijun You [a,b,*], Pedro Fardim [d]

[a] School of Food Science and Engineering, South China University of Technology, Guangzhou, Guangdong 510640, China
[b] Overseas Expertise Introduction Center for Discipline Innovation of Food Nutrition and Human Health (111 Center), Guangzhou 510640, Guangdong, China
[c] Department of Pediatrics, the Affiliated Hospital of South China University of Technology, Guangzhou, Guangdong 510640, China
[d] Chemical Engineering for Health & Care, Bio & Chemical Systems Technology, Reactor Engineering and Safety, Department of Chemical Engineering, KU Leuven, Belgium

ARTICLE INFO

Keywords:
Gracilaria lemaneiformis
Sulfated polysaccharide
Anti-inflammatory activity
Tight junction

ABSTRACT

This study was aimed to characterize *Gracilaria lemaneiformis* polysaccharides and evaluate their protective effects on Lipopolysaccharide-induced injury in IEC-6 cells. The *G. lemaneiformis* polysaccharide was degraded by UV/H_2O_2 treatment and purified to three fractions named GLP-1.0 M, GLP-1.4 M and GLP-1.6 M. The purified fractions were mainly composed of galactose, glucose and xylose. The structural analysis showed that GLP-1.6 M was a typical sulfated red alga polysaccharide containing the linear backbone of β-(1 → 3)- and α-(1 → 4)-linked galactosyl residues, anhydro-galactose units. In the Lipopolysaccharide-induced IEC-6 cells model, GLP-1.6 M exerted the strongest *in vitro* anti-inflammatory activity by inhibiting the release and expressions of tumor necrosis factor-α, interleukin-6 and interleukin-1β by 89.93%, 67.82% and 38.06%, respectively. Meanwhile, GLP-1.6 M enhanced the intestinal barrier function via up-regulating the expressions of tight junctions and mucin. Therefore, the purified polysaccharide from *G. lemaneiformis* could be a promising candidate for maintaining intestinal health in the food and pharmaceutical industries.

1. Introduction

Inflammation, the first response of the body's immune system, is a physiological phenomenon in the event of injury, infection and stress. Inflammation is a natural protective response featured by the migration of proliferating leucocytes from blood to tissues and a series of signaling molecules involved, including nitric oxide (NO), tumor necrosis factor-a (TNF-α), interleukin-6 (IL-6) and interleukin-1β (IL-1β), whose accumulation indicates the generation of inflammation response (Cheng, Chao, Chang, & Lu, 2016). However, prolonged and chronic inflammation could lead to various diseases, such as fever, asthma, atherosclerosis and even cancer (Graham & Xavier, 2020). What's more, intestinal inflammation is a major health issue that generally occurred in the intestine and colon that induces a series of intestinal diseases including inflammatory bowel disease (IBD) and irritable bowel syndrome (IBS) (Zhuang, Zhong, Zhou, Zhong, Liu, & Liu, 2019).

Additionally, intestinal inflammation has been verified to be related to the intestinal epithelial barrier disruption. Intestinal epithelial barrier, a mechanical barrier of resisting the invasion of extrinsic substances, consists of intestinal epithelial cells and junction complex (Liu et al., 2020). Destruction of intestinal barrier increases the permeability and causes intestinal mucosal inflammation (Okumura & Takeda, 2018). An extremely united mucosal barrier system is established by tight junctions and mucins together, which could maintain the mechanical barrier and permeability of intestinal epithelium via resisting the invasion of extrinsic substances (Li et al., 2021). Moreover, lipopolysaccharide (LPS) is from the outer wall of Gram-negative bacteria, which is considered as a common stimulus to induce inflammation in intestinal epithelial cells via activating chemical mediators (e.g., NO, TNF-α, IL-6 and IL-1β) and destroying the intestinal barrier; (Singh et al., 2018).

The sulfated polysaccharide from red seaweeds *Gracilaria lemaneiformis* (*G. lemaneiformis*) have been proved to possess diversified functions, such as hypolipidemic, immune regulation, gut microbiota modulation, colitis prevention and so on (Li et al., 2020). However,

* Corresponding author at: School of Food Science and Engineering, South China University of Technology, 381 Wushan Road, Guangzhou 510640, China.
E-mail address: feyoulijun@scut.edu.cn (L. You).
[1] These two authors contributed equally to this article.

https://doi.org/10.1016/j.fochx.2021.100157
Received 21 July 2021; Received in revised form 21 October 2021; Accepted 8 November 2021
Available online 9 November 2021

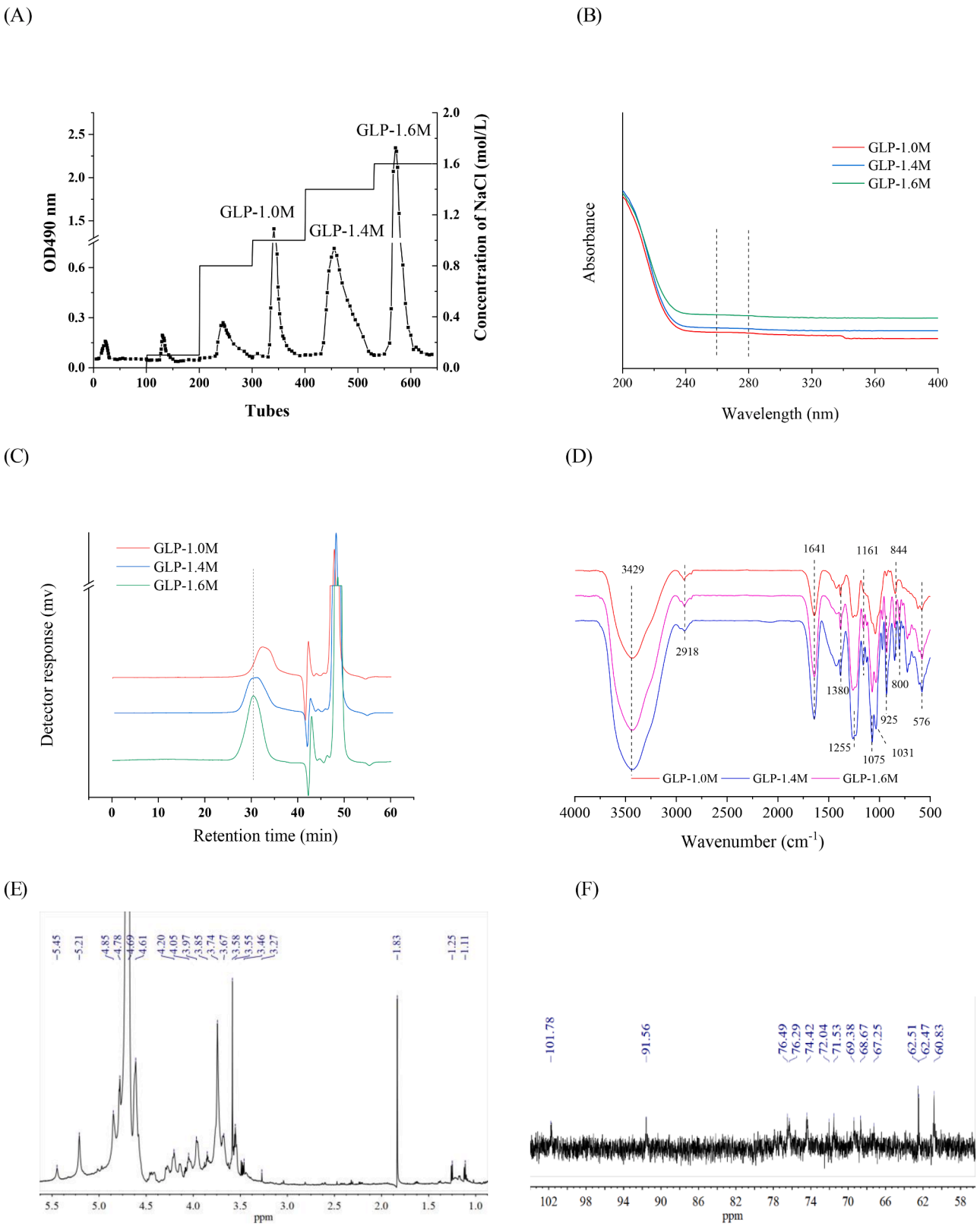

Fig. 1. The DEAE column chromatography elution curve of 5-GLP (A); UV spectra (B); The molecular weight distribution (C) and FT-IR spectra (D) of purified fractions of *G. lemaneiformis* polysaccharides; ^{1}H NMR (E) and ^{13}C NMR (F) of GLP-1.6 M.

G. lemaneiformis polysaccharide (GLP) extracted by hot water normally present low solubility and high gelling properties. Our previous study implied that UV/H2O2 treatment could decrease the viscosity of GLP, and improve its anti-inflammatory activity in the LPS-induced IEC-6 cells model. The aim of this study is to find out the active components of 5-GLP and its possible anti-inflammatory mechanism. Therefore, three different purified fractions were separated and characterized from the degradation product 5-GLP from *G. lemaneiformis* polysaccharide with

UV/H_2O_2 treatment. Furthermore, the protective effects of purified polysaccharides on intestinal barrier were investigated using the LPS-induced IEC-6 cells model.

2. Materials and methods

2.1. Materials and reagents

Dulbecco's modified Eagle's medium (DMEM), fetal bovine serum (FBS), insulin, penicillin and streptomycin were purchased from GIBCO (Carlsbad, CA, USA). LPS and dextran standards (4.32, 12.6, 126 and 289 kDa) were purchased from Sigma Aldrich Chemical Co. (St. louis, MO, USA). 3-(4, 5-dimethylthiazol-2-yl)-2, 5-diphenyltetrazolium bromide (MTT) was purchased from Nanjing Jiancheng Bioengineering Institute (Nanjing, Jiangsu, China).

2.2. Preparation and purification of polysaccharide from Gracilaria lemaneiformis

The polysaccharide from *G. lemaneiformis* (Weihai, Shandong, China) was prepared using hot water extraction as previously described (Gong et al., 2021). Coarse powder was refluxed with 95% ethanol twice (for 3 and 1 h, respectively) to remove small molecular substance including lipids and pigments after superfine pulverization. The dried powder (100 g) was extracted using boiling water (5 L) for 2 h. After centrifugation (8000 *g*, 20 min) and concentration, the ethanol was added to a concentration of 80% for alcohol precipitation at 4 °C overnight. The crude polysaccharide (named GLP) was obtained after freeze-drying. According to our previous report (Gong et al., 2021), GLP (25 mL, 12 mg/mL) was further treated using H_2O_2 (5 mL, 300 mM) and UV radiation (6500 mJ/cm^2) for 5 min by an apparatus HOPE-MED 8140 (Tianjin Hepu Industry and Trade Co., Tianjin, China). After concentrated and dialysis (molecular weight cut-off of 500 Da), the degradation product was obtained and named as 5-GLP. The degradation product was further purified by an anion-exchange chromatography of DEAE Fast Flow with NaCl solution (0.1–1.6 mol/L) as the eluent at a flow rate of 2.0 mL/min. Each tube with 5 mL of eluent was collected to detect the content of total sugar. According to the result, the three purified fractions obtained by 1.0 M, 1.4 M and 1.6 M NaCl elution were collected and dialyzed (Mw cut off 3000 Da), named as GLP-1.0 M, GLP-1.4 M and GLP-1.6 M, respectively (Fig. 1A).

2.3. Chemical composition of polysaccharides

The contents of total sugar, uronic acids and sulfate in the purified fractions were detected using the phenol–sulfuric acid method, the carbazole sulfuric acid method and the barium sulfate turbidimetry method, respectively, as previously described (Gong et al., 2021).

2.4. Distribution of molecular weight (Mw)

The molecular weights of purified fractions were measured using high pressure gel permeation chromatography. The purified fractions (2 mg/mL) were dissolved in mobile phase (0.02 M KH_2PO_4), filtered through 0.22 μm filter membrane and applied to a TSK-GEL guard column (6.0 × 40 mm), a TSK $G6000_{PWXL}$ column (7.8 × 300 mm) and a TSK $G3000_{PWXL}$ column (7.8 × 300 mm) (Tosoh Co., Tokyo, Japan) in series at 35 ± 1 °C. And sample was eluted with mobile phase into a Waters 2414 system (Waters Co., Milford, MA, USA) at 0.5 mL/min. Dextran standards were calibrated as the linear regression.

2.5. UV spectra

Purified fractions (0.1 mg/mL) were dissolved in ultrapure water (ultrapure water as the blank). The UV spectra were determined in the range of 200–400 nm using a DU 730 Nucleic Acid/Protein Analyzer (Beckman Coulter Co., Fullerton, California, USA).

2.6. Structural characteristics analysis

2.6.1. Monosaccharide composition of polysaccharides

The monosaccharide compositions of purified fractions were determined according to other previous reports (Chen, You, Abbasi, Fu, & Liu, 2015) using ion exchange chromatography (Dionex ICS 3000). In a serum bottle, sample was dissolved in trifluoroacetic acid (2 M, m/v = 2:1) and reacted at 105 °C for 6 h. Then, excess trifluoroacetic acid was removed using a rotary evaporation under reduced pressure at 60 °C with methanol for five times. The hydrolyzed sample was re-dissolved in ultrapure water, filtered through 0.22 μm filter membrane and applied to a CarboPac PAI (250 × 4 mm, id. 5 μm, Dionex, Thermo Fisher Scientific Co., Waltham, Massachusetts, USA) with a gradient elution by water/NaOH at a flow rate of 0.5 mL/min at 30 °C.

2.6.2. Fourier transform infrared (FT-IR) spectra analysis

The IR analysis were done using a Tensor 27 FT-IR spectrophotometer (Bruker, Bergisch, Gladbach, Germany). The mixture of KBr granules and purified fractions at the ratio of 100:1 (w/w) were prepared and measured in the wavelength range from 4000 to 4000 cm^{-1}.

2.6.3. Scanning electron microscope (SEM) analysis

The surface topographies of purified fractions were measured using an EVO 18 SEM (Carl Zeiss AG, Oberkohen, Baden-Wurttemberg, Germany) at an acceleration voltage of 5 kV. The powder of purified fractions was covered with gold layer and observed with the magnifications of 1000 × and 2000 x.

2.6.4. Atomic force microscopy (AFM) analysis

The purified fractions (10^{-5} mg/mL) were completely dissolved in ultrapure water. After filtered through 0.22 μm water membrane, 2–3 μL of aqueous solution was deposited onto a freshly cleaved mica plate and dried at room temperature. AFM was operated using the ScanAsyst-mode. Images of the purified fraction were acquired by a Nanoscope llla equipment (Bruker, Bergisch Gladbach, Germany) and obtained using the software NanoScope Analysis (Version 1.7).

2.6.5. Nuclear magnetic resonance (NMR)

GLP-1.6 M (20 mg) was dissolved with 0.55 mL deuterated water (D_2O, Macklin, Shanghai, China) in an NMR tube after lyophilized 2–3 times in D_2O. ^1H and ^{13}C NMR spectra were acquired on a Bruker AVANCE III HD 600 spectrometer (Bruker Co., Billerica, MA, USA). The NMR data were analyzed using MestReNova 11.0 software (Bruker Co., Bergisch Gladbach, Germany).

2.7. Protective effects of polysaccharide on IEC-6 cells

2.7.1. Cell culture

The IEC-6 intestinal epithelial cell line was obtained from Kunming Cell Bank, Chinese Academy of Sciences (Lot No. KCB200720YJ) and was cultured in DMEM containing 10% FBS, 0.1 IU/mL insulin and 1% penicillin–streptomycin at 37 °C under a 5% CO_2 atmosphere.

2.7.2. Viability assay

Cell viability was measured by MTT assay. In brief, the IEC-6 cells were grown in a 96-well plate at a density of 1 × 10^4/well for 24 h and pre-treated with DMEM containing different concentrations of purified fractions (ranging from 0 to 800 μg/mL) for 24 h. Then treated cells in each well were added with 50 μL of 1 × MTT solution, incubated at 37 °C for 4 h and were added with 150 μL DMSO. Cells cultured without polysaccharide treatment was considered as the control group. The absorbance was recorded at a wavelength of 570 nm using a microplate reader (FilterMax F5, Molecular Devices Co, San Francisco, California, USA). Cell viability was represented by the absorbance of treated groups

Table 1
The chemical compositions of purified fractions.

Content/%	GLP-1.0M	GLP-1.4M	GLP-1.6M
Total sugars	51.28 ± 0.08 [a]	50.69 ± 0.77 [a]	48.95 ± 1.18 [a]
Uronic acids	5.86 ± 0.71 [a]	4.52 ± 0.13[b]	4.51 ± 0.52[b]
Sulfate	21.35 ± 0.77 [a]	24.56 ± 0.80[b]	30.92 ± 0.08[c]
Monosaccharide molar ratio			
Fucose	1.52	0.70	0.67
Galactose	64.76	90.21	37.88
Glucose	4.90	0.99	28.61
Xylose	25.47	7.33	27.74
Mannose	–	–	0.20
Arabinose	–	–	2.12
Galacturonic acid	1.05	0.26	1.91
Glucuronic acid	2.30	0.51	0.87

Data are shown as mean ± SD with n = 3 with different superscripts indicate significant difference among the means with $P < 0.05$ by one-way ANOVA and Duncan test.

relative to that of the control group.

2.7.3. Nitric oxide (NO) content determination

The IEC-6 cells were pre-treated in a 6-well plate at a density of 1×10^6/well for 24 h with or without GLPs (5-GLP, GLP-1.0 M, GLP-1.4 M and GLP-1.6 M) at 50, 100 and 200 μg/mL for 6 h, respectively. After pre-treatment, LPS (final concentration of 100 μg/mL,) was added to each well (except the control) for 24 h. Then the concentration of NO in the cell culture supernatants was detected using a NO determination kit (Beyotime Biotechnology, Co., Shanghai, China) by the Griess Reagent colorimetric method (Wilms, Sievers, Rickert, Rostami-Yazdi, Mrowietz & Lucius, 2010) at 540 nm.

2.7.4. The contents of inflammatory cytokines

The medium was collected and centrifuged according to section 2.7.3. Then the contents of inflammatory cytokines including TNF-α, IL-6 and IL-1β, were measured using corresponding ELISAD kits (Multi Sciences Biotech, Co., Zhejiang, Hangzhou, China and Neobioscience Technology Co., Shenzhen, Guangdong, China) according to the manufacturer's instructions.

2.7.5. Real-time quantitative PCR (RT-qPCR)

The IEC-6 cells were seeded in a 6-well plate at a density of 1×10^6/well and treated according to section 2.3.7. The cells were cracked using trizol reagent (Thermo Fisher Scientific Co., New York, USA). Cells' total RNA was extracted using Trizol Assay (Bo et al., 2021). Total RNA was reversed to cDNA using REVERTAID 1^{ST} CDNA SYNTH KIT EA (Thermo Fisher Scientific) by $T100^{TM}$ Thermal Cycler (Bio-Rad, Hercules, CA, USA). RT-qPCR was performed using Mini $Opticon^{TM}$ Detector (CFD-3120, Bio-Rad). The qPCR program was as follows: 1 cycle of 95 °C for 10 min, followed by 40 cycles of 95 °C for 15 s and 60 °C for 1 min, then followed by melting curve analysis to determine the product specificity from 65 °C to 95 °C with 0.5 °C increments at 5 s per step. The expression levels of target genes were normalized to the reference gene GAPDH and calculated with the $2^{-\Delta\Delta Ct}$ method (Adam, Drewnowski, S, & Specter, 2004). The primer sequences (Sangon Biotech, Shanghai, China) used in RT-qPCR were listed in Table S1.

2.8. Statistical analysis

Data were presented as mean ± standard deviation (SD). Statistical comparison was tested using one-way (ANOVA) analysis followed by Duncan's multiple range tests with SPSS Statistics 17 (IBM Corp., Armonk, NY, USA).

3. Results and discussion

3.1. Chemical compositions of purified fractions

As shown in Fig. 1A, the degraded production (5-GLP) was isolated and purified using an anion-exchange chromatography of DEAE Fast Flow. Three major fractions named GLP-1.0 M, GLP-1.4 M and GLP-1.6 M were obtained with the yield of 8.95%, 10.56% and 21.37%, respectively. In Table 1, the content of total sugar (51.28 ± 0.08%) in GLP-1.4 M was the highest. When the concentration of NaCl increased, the contents of sulfate in purified fractions increased, while the contents of uronic acids decreased. GLP-1.6 M had the highest content of sulfate (30.92 ± 0.08%) and the lowest content of uronic acids (4.51 ± 0.52%). Meanwhile, the UV spectra showed that there was few protein and nuclear acid in these purified fractions (Fig. 1B), which meaned that polysaccharides and the attached sulfates are the main components of GLP-1.0 M, GLP-1.4 M and GLP-1.6 M.

3.2. Molecular weight analysis

As shown in Fig. 1C, GLP-1.6 M was a homogeneous polysaccharide with a sharp peak, while GLP-1.0 M and GLP-1.4 M were not. On the basis of the equation of calibration curve, the average molecular weights of GLP-1.0 M, GLP-1.4 M and GLP-1.6 M were calculated as 94.48, 172.85 and 250.39 kDa, respectively. In the preliminary experiments, three purified fractions eluted from 0 M, 0.1 M and 0.8 M NaCl were not considered for the further tests due to their low yields and poor anti-inflammatory activities.

3.3. Monosaccharide composition

In Table 1, three purified fractions (GLP-1.0 M, GLP-1.4 M and GLP-1.6 M) possessed similar monosaccharides (fucose, galactose, glucose, xylose, galacturonic acid and glucuronic acid) with different ratios. Distinctly, galactose, glucose and xylose were the main components. The contents of galactose were the highest in all purified fractions as 64.76% in GLP-1.0 M, 90.21% in GLP-1.4 M and 37.88% in GLP-1.6 M, respectively. Especially, the ratios of monosaccharides in GLP-1.6 M were different from those in the other two purified fractions (GLP-1.0 M and GLP-1.4 M). The molar ratio percentage of galactose, glucose and xylose, arabinose, galacturonic acid, glucuronic acid, fucose and mannose in GLP-1.6 M were 37.88%, 28.61%, 27.74%, 2.12%, 1.91%, 0.87%, 0.67% and 0.20%, respectively. This indicated that the biological activity may show differences because of it. Meanwhile, the monosaccharide compositions of polysaccharides were reported to be closely related to their biological activities (You, Gong, Li, Hu, Brennan, & Kulikouskaya, 2020), and the intestinal flora was one of the most direct targets.

3.4. FT-IR spectra analysis

As shown in Fig. 1D, three purified fractions possessed similar characteristic absorption bands. The strong absorption peak at 3429 cm^{-1} was a typical O—H bending vibration. The weak absorption bands at 2918 cm^{-1} and 1380 cm^{-1} were derived from the C—H stretching and bending vibration, respectively (Sen & Erboz, 2010). The absorption bands at 1255 cm^{-1} and 576 cm^{-1} were attributed to the S═O stretching and bending vibration, respectively. Combined with an absorption band at 844 cm^{-1} originated from the C—O—S stretching vibration, the three bands suggested the existence of sulfate in the purified fractions (Volery, Besson, & Schaffer-Lequart, 2004). In addition, the absorption bands at 1161 cm^{-1}, 1075 cm^{-1} and 1031 cm^{-1} were due to the presence of galactose and glucose in purified fractions (Yu et al., 2015). The absorption bands at 925 cm^{-1} and 800 cm^{-1} represented the existence of β-glycosidic and α-glycosidic configuration, respectively (Chen, You, Abbasi, Fu, & Liu, 2015). Obvious inverted peaks could be

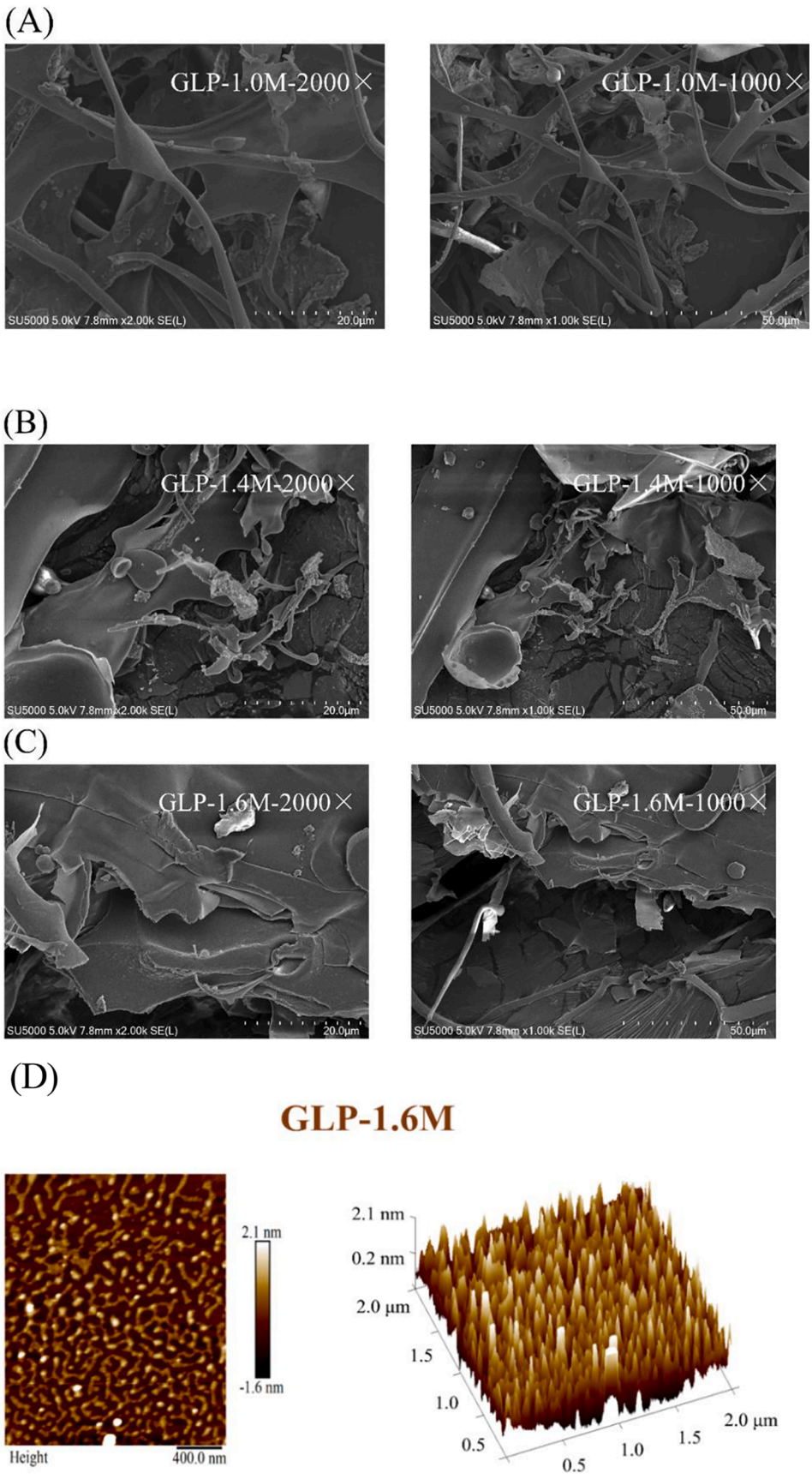

Fig. 2. SEM spectra of purified fractions: GLP-1.0 M (A); GLP-1.4 M (B); GLP-1.6 M (C) and AFM 2D & 3D images (D).

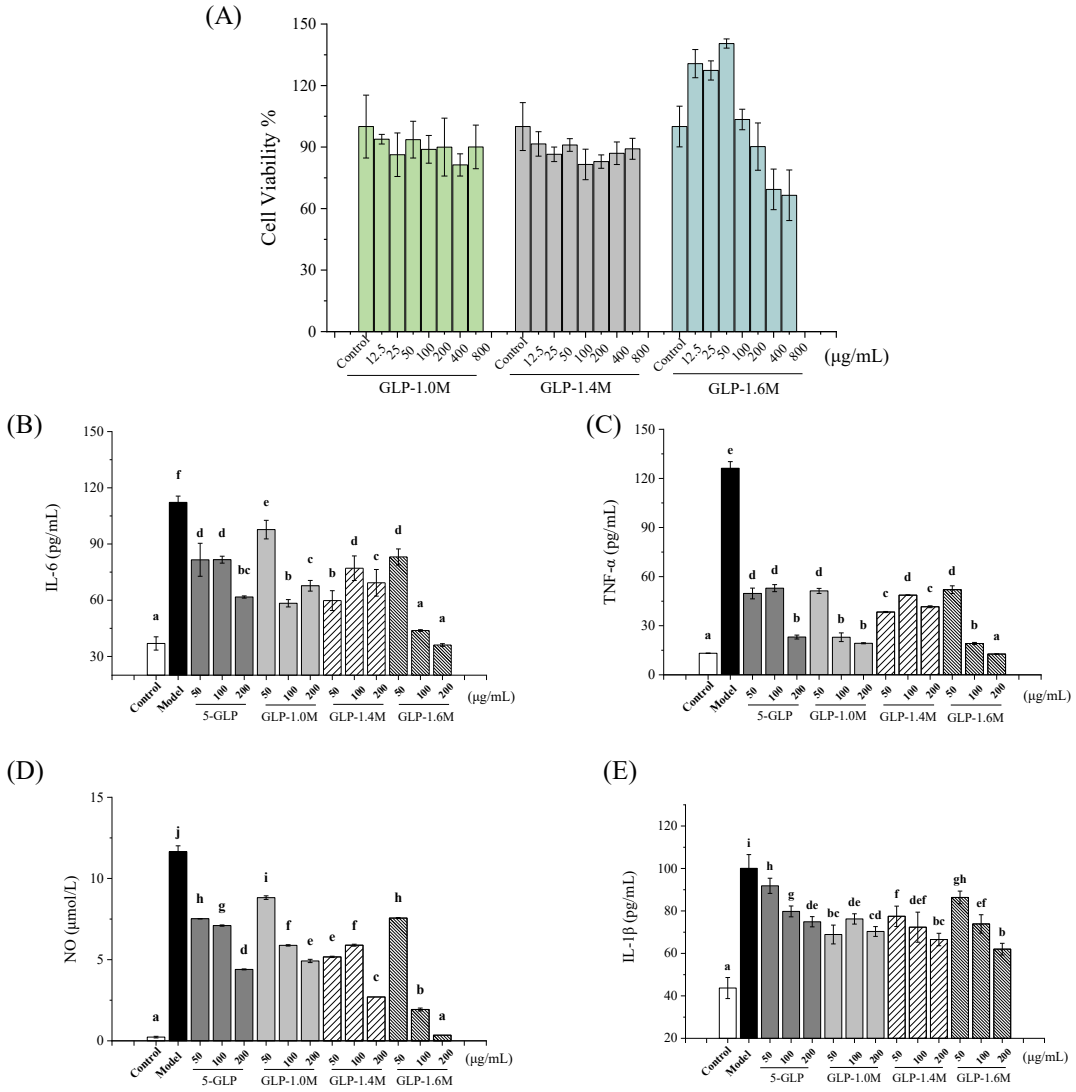

Fig. 3. Cell viability (A); The effects on the secretion of NO (B); TNF-α (C); IL-6 (D) and IL-1β (E) of purified fractions. Data are shown as mean ± SD with n =3 with different superscripts indicate significant difference among the means with $P < 0.05$ by one-way ANOVA and Duncan test.

observed in both GLP-1.2 M and GLP-1.6 M at 925 cm^{-1} while only a small inverted peak was in GLP-1.0 M, indicating that the content of α-glycosidic bond might be higher than that of β-glycosidic bond in GLP-1.0 M. The results suggested that GLP-1.0 M, GLP-1.4 M and GLP-1.6 M were sulfated polysaccharides with structural differences, consistent with the result of chemical composition.

3.5. SEM measurements analysis

SEM analysis revealed the surface topographies (1000 × and 2000 x) of the purified fractions (GLP-1.0 M, GLP-1.4 M and GLP-1.6 M). As shown in Fig. 2, GLP-1.0 M, GLP-1.4 M and GLP-1.6 M had significant variation in surface appearance. GLP-1.0 M presented a microstructure of strips and flakes. GLP-1.4 M showed an image of large and smooth flakes with part of strips. The smoothness of microstructure surface was related to the characteristic feature of sulfated polysaccharides (Krol, Malik, Marycz, & Jarmoluk, 2016). GLP-1.6 M presented an image of thick flakes with the attachment of massive particles and strips.

3.6. AFM images analysis

GLP-1.6 M was selected for further analysis by AFM and NMR due to its higher yield and stronger anti-inflammatory activity compared with GLP-1.0 M and GLP-1.4 M. As illustrated in Fig. 2D, the curved and stubby chains of surface morphology were shown from the AFM 2D image, which was consistent with the result of a sulfated polysaccharide from red seaweed (*Porphyra haitanensis*) (Khan, Qiu, Xu, Liu, & Cheong, 2020). The heights of lumps and particles were 2.1 nm and 0.2 nm, respectively greatly different from those of 5-GLP based on our previous report (Gong et al., 2021). The conformation was transformed from irregular spherical lumps to curved chains. Some previous studies showed that the conformations of polysaccharides were closely related to their biological activities. For example, sea cucumber fucoidans with chains conformation exerted better gastric protective activities (Xu, Chang, Xue, Wang, & Shen, 2018). The conformation of curved chains in GLP-1.6 M might be a reason for the stronger anti-inflammatory activity.

3.7. NMR spectroscopy analysis

NMR spectroscopy is an effective method to analyze the structural configurations of polysaccharides. GLP-1.6 M showed a complex ^{1}H spectrum (Fig. 1E). The anomeric resonances at δ 5.21 and δ 4.61–4.85 suggested the existence of α-(1 → 4)- and β-(1 → 3)-linked galactopyranosyl units, respectively (Aquino, Landeira-Fernandez, Valente, Andrade, & Mourao, 2005; Bilan, Vinogradova, Shashkov, & Usov, 2007; Lahaye, Revol, Rochas, McLachlan, & Yaphe, 1988; Murano,

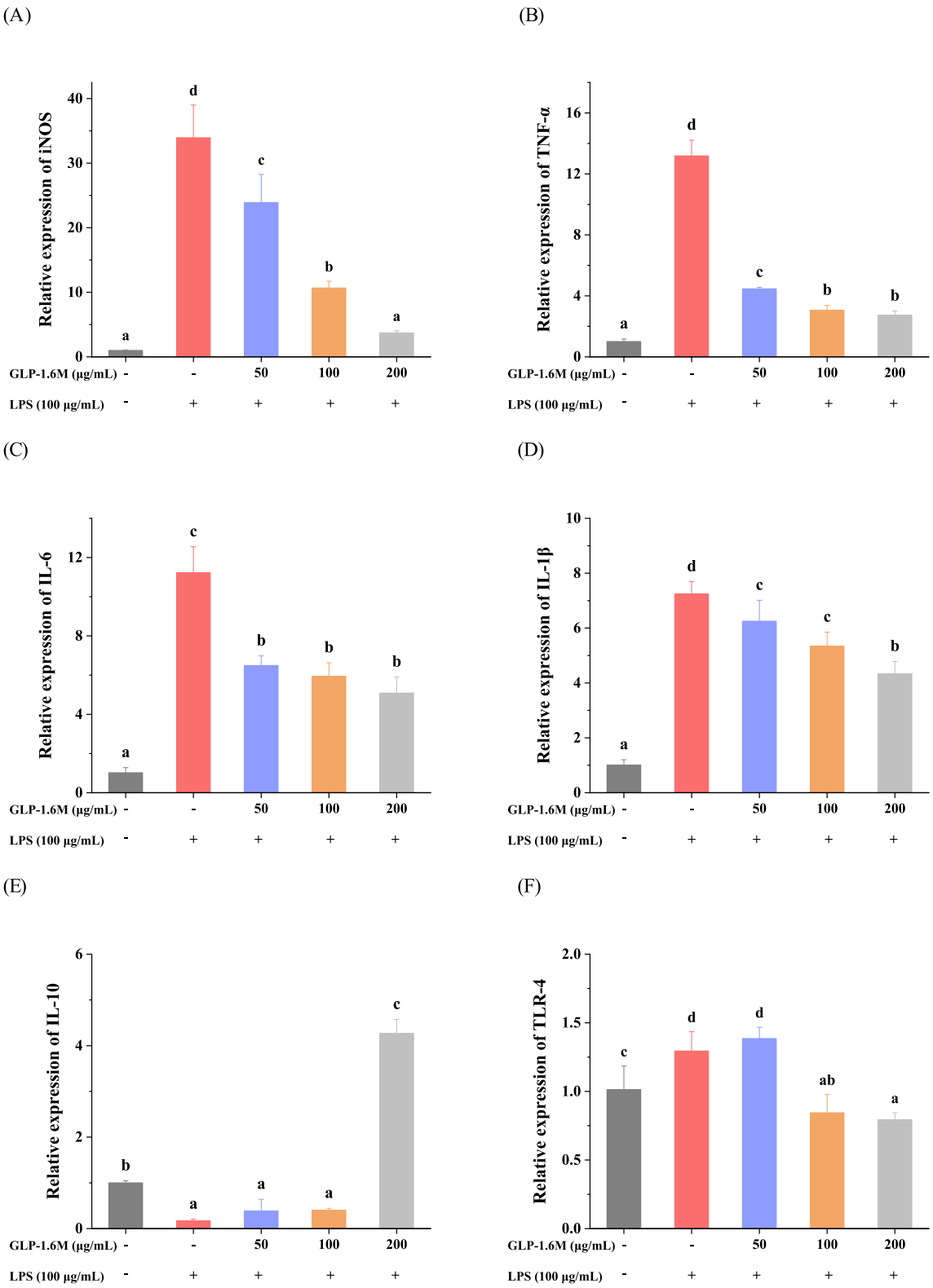

Fig. 4. The relative expressions of iNOS (A); TNF-α (B); IL-6 (C); IL-1β (D); IL-10 (E) and TLR-4 (F) in IEC-6 cells, and the relative expressions of ZO-1 (G); Occludin (B); Claudin-1 (C) and MUC-2 (D) in IEC-6 cells. Data are shown as mean ± SD with n =3 with different superscripts indicate significant difference among the means with $P < 0.05$ by one-way ANOVA and Duncan test.

Toffanin, Zanetti, Knutsen, Paoletti, & Rizzo, 1992). It indicated that the content of β-glycosidic bond was higher than that of α-glycosidic bond and this result was consistent with the FT-IR result. Moreover, the (1 → 3)- and (1 → 4)-linked galactosyl residues in the sulfated galactan of marine red macroalgae were generally in correspondence to β-and α-linked, respectively (Chattopadhyay, Ghosh, Pujol, Carlucci,

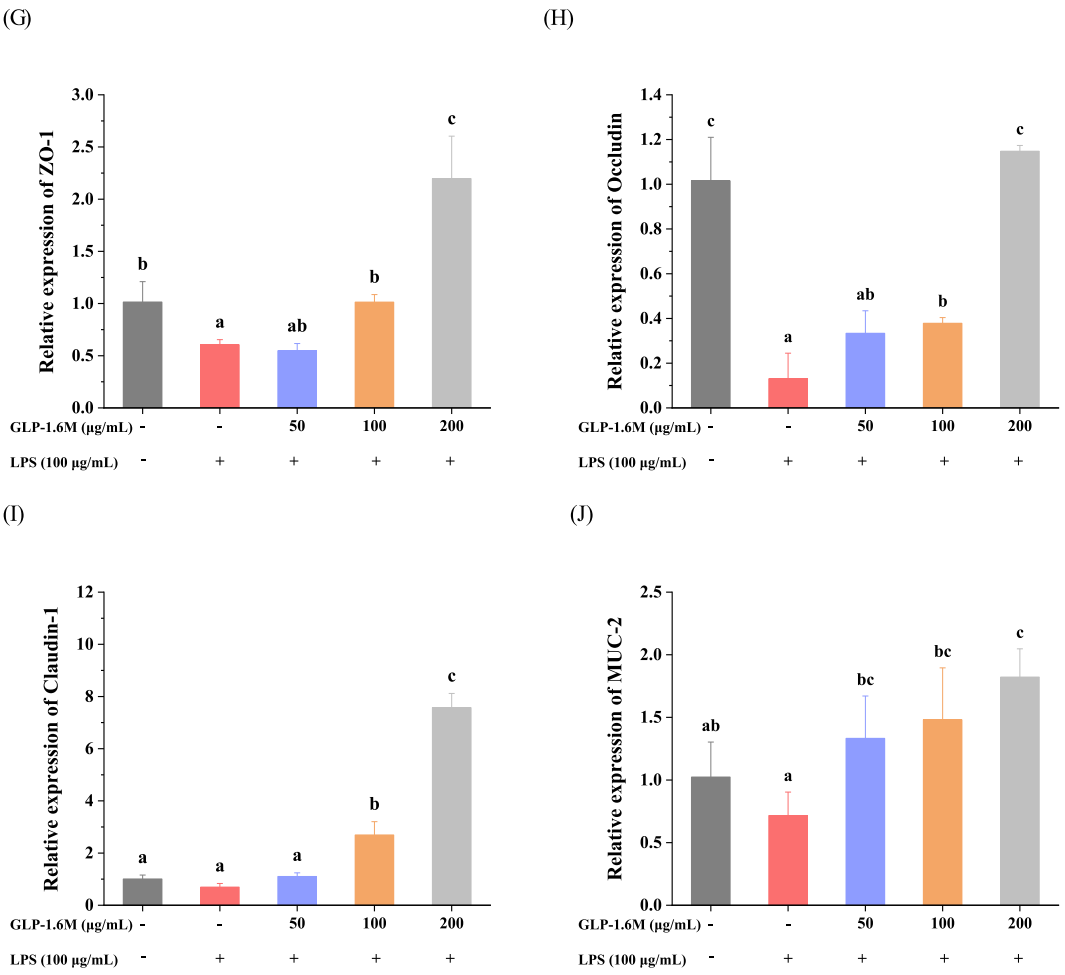

Data are shown as mean ± SD with n =3 with different superscripts indicate significant difference among the means with $P < 0.05$ by one-way ANOVA and Duncan test.

Fig. 4. (*continued*).

Damonte, & Ray, 2008). The high intensity sharp signal at δ 3.58 in the ^{1}H NMR spectrum was tentatively attributed to the methoxy group of 2-O-methyl α-(1 → 4)-linked-3,6-anhydro-galactose (Murano et al., 1992). The ^{1}H NMR signals at δ 5.21 and δ 3.74 were related to the anomeric signals of 3,6-anhydro-α-galactose residues and the existence of ι-carrageenan with sulfate, respectively (Li et al., 2020; Aquino et al., 2005; Farias, Valente, Pereira, & Mourao, 2000). GLP-1.6 M showed a ^{13}C NMR spectrum of typical polysaccharides (signals at δ 60–102) (Fig. 1F). It contained more than 10 signals, including signals at δ 101.78 and δ 91.56, which could be observed in the anomeric carbon resonance zone of the polysaccharide (Khan et al., 2020). It might well illustrate the presence of sulfated polysaccharides. The ^{13}C NMR and ^{1}H NMR spectra signals at δ 101.78 (4.61) were typical signals of the C-1 (H-1) galactose residues (Khan et al., 2020). The ^{13}C NMR signal at δ 91.56 was a specific signal of the α anomeric form of 3, 6-anhydro-galactose units (Gen et al., 2015). In conclusion, GLP-1.6 M was a typical sulfated red alga polysaccharide, containing the linear backbone of β-(1 → 3)- and α-(1 → 4)-linked galactosyl residues, anhydro-galactose unitsxs. This result was similar to some previous reports about *Gracilaria lemaneiformis* polysaccharide.(Li et al., 2020; Veeraperumal et al., 2020)

3.8. The viability of IEC-6 cells

As shown in Fig. 3A, GLP-1.0 M and GLP-1.4 M did not have significant cytotoxic effects at 12.5–800 μg/mL for 24 h, while GLP-1.6 M had significant cytotoxic effect at 400 and 800 μg/mL. Based on the above result and our previous report,(Gong et al., 2021) safe doses of all polysaccharide (GLP-1.0 M, GLP-1.4 M, GLP-1.6 M and 5-GLP) were set at 50, 100 and 200 μg/mL for the following tests.

3.9. The effects on production of NO and inflammatory cytokines

The LPS-induced IEC-6 cells model was used to evaluate the anti-inflammatory activities of four polysaccharide samples (GLP-1.0 M, GLP-1.4 M, GLP-1.6 M, and 5-GLP). As shown in Fig. 3B-E, compared with the control group, LPS stimulation significantly increased the production of NO, TNF-α, IL-6 and IL-1β by 50.65, 8.57, 2.04 and 1.29 folds, respectively ($p < 0.05$). Compared with the model group, all the polysaccharide treated groups inhibited the production of NO and inflammatory cytokines ($p < 0.05$). The commonality of the three samples indicates that the sulfate group may play an important role in the above activities. Particularly, GLP-1.6 M showed the strongest *in vitro* anti-inflammatory activity. It inhibited the secretion of NO, TNF-α, IL-6 and IL-1β in a dose-dependent manner by 97.00%, 89.93%, 67.82%

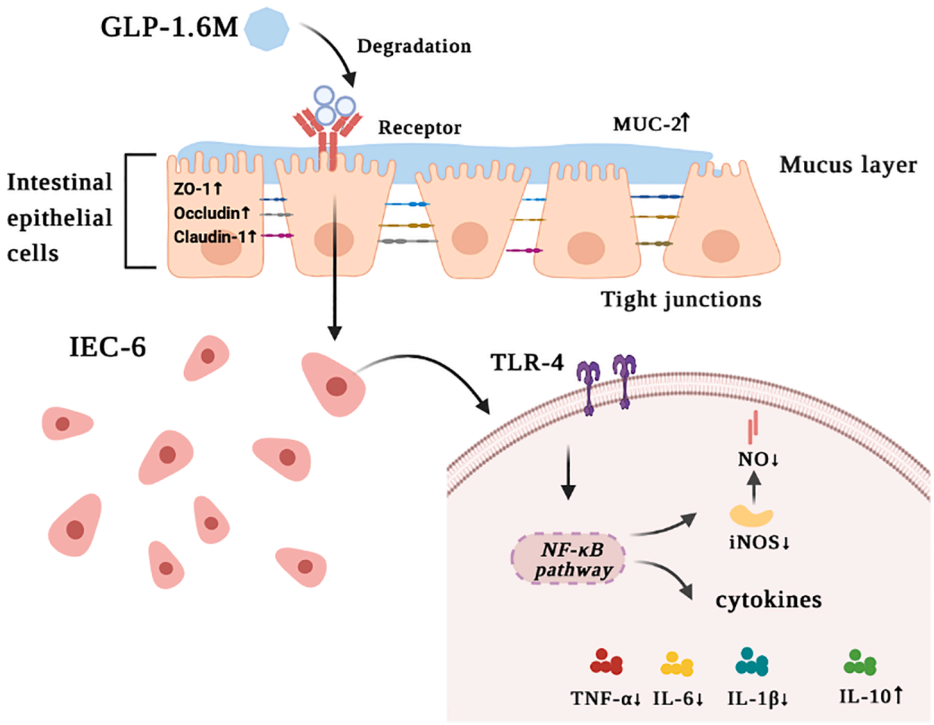

Fig. 5. Brief sketch of mechanism in anti-inflammatory effect of GLP-1.6 M.

and 38.06% at 200 μg/mL, respectively. Associated with the results of chemical composition, higher sulfate might be the main reasons for its better activity. Studies have shown that higher sulfate can improve the antioxidant and immune activities of polysaccharides (Jiao, Yu, Zhang & Ewart, 2011; Qi et al., 2005). Higher molecular weight and relative content of glucose residues might be the other reasons. Therefore, GLP-1.6 M was selected for the further study in the expressions of related genes and the analysis of structural configuration.

NO was considered as an important mediator in the inflammatory response produced by the stimulation of inducible nitric oxide synthase (iNOS). The pro-inflammatory cytokines (TNF-α, IL-1β and IL-6) in intestinal epithelial cells played a crucial role in intestinal inflammation, which were accumulated in inflammation and tissue damage (Niu et al., 2021). TNF-α was reported to induce intestinal barrier damage and inflammation of IEC-6 cells (Zhuang et al., 2019). Lowering the levels of NO and pro-inflammatory cytokines was generally considered to have stronger anti-inflammatory activity (Lee, Sudjarwo, Kim, Dirgantara, Maeng, & Hong, 2014). Therefore, these results indicated that *G. lemaneiformis* polysaccharide exerted anti-inflammatory activities by inhibiting the production of NO and pro-inflammatory cytokines including TNF-α, IL-1β and IL-6.

3.10. The effects on the relative expressions of inflammation-related genes

As shown in Fig. 4A-F, compared with the control group, LPS stimulation significantly increased the expressions of iNOS, TNF-α, IL-6, IL-1β and TLR-4 (Toll-like receptor 4) by 32.88, 12.07, 9.98, 6.16 and 0.28 folds and decreased the expression of IL-10 by 0.83 folds, respectively ($p < 0.05$). Compared with model group, GLP-1.6 M (200 μg/mL) inhibited the expressions of iNOS, TNF-α, IL-6, IL-1β and TLR-4 by 89.05%, 79.25%, 54.69%, 40.18%, 38.46% and promoted the expression of IL-10 at 24.12 folds, respectively ($p < 0.05$). Especially, the high dose of GLP-1.6 M exerted the strongest effects on attenuating the damage of intestinal barriers by improving the expressions of inflammation-related genes.

The inflammatory response was involved in some signaling molecules. iNOS was a main enzyme responsible for LPS-induced NO production (Du, Lin, Bian, & Xu, 2015; Mueller, Hobiger, & Jungbauer, 2010). TLR-4 was a receptor for responding to LPS (Fitzgerald & Kagan, 2020). After a response, TLR-4 could activate a series of pathways and eventually activate NF-κB pathway to promote the production of pro-inflammatory cytokines, such as IL-6 and IL-1β (Vidya, Kumar, Sejian, Bagath, Krishnan, & Bhatta, 2018). Inhibiting the expressions of iNOS and TLR-4 could alleviate the LPS-induced inflammation. In addition, the sulfated polysaccharide was reported to block the inflammatory signal transduction binding to TLR-4 (Chen, Wu, & Wen, 2008). IL-10 was considered as a typical anti-inflammatory cytokine participating in the inflammation response (Gandhi et al., 2020). In our study, GLP-1.6 M exhibited stronger anti-inflammatory activity by down-regulating the expressions of iNOS, TLR-4 and pro-inflammatory cytokines (TNF-α, IL-6 and IL-1β) and up-regulating the expression of anti-inflammatory cytokine (IL-10), which might be involved in TLR-4/NF-κB pathway (Li, Duan, Li, Pan, & Han, 2021).

3.11. The effects on the relative expressions of tight junctions-related genes

As shown in Fig. 4G-J, compared with the control group, LPS stimulation obviously decreased the expressions of MUC-2 and TJs (ZO-1, Occludin and Claudin-1) by 30%, 40.37%, 87.12% and 30.95%, respectively ($p < 0.05$). Compared with model group, GLP-1.6 M significantly up-regulated the relative expressions of MUC-2 and TJs in a dose-dependent manner. GLP-1.6 M (100 and 200 μg/mL) up-regulated the expression of MUC-2 by 1.06 and 1.53 folds, respectively ($p < 0.05$). GLP-1.6 M (200 μg/mL) also up-regulated the levels of TJs (ZO-1, Occludin and Claudin-1) by 2.6, 9.82 and 7.82 folds, respectively ($p < 0.05$). Moreover, the level of Occludin in GLP-1.6 M treated group at high dose was almost closed to that in the control group ($p < 0.05$). The levels of MUC-2, ZO-1 and Claudin-1 in GLP-1.6 M treated group were significantly higher than those in the control group ($p < 0.05$).

Tight junctions were reported to play an indispensable role in the intestinal barrier and its lower level indicated the disruption of intestinal barrier (Zhao, Li, Sun, Su, Geng, & Sun, 2020). ZO-1 was considered as a critical tight junction protein, which was widely used to evaluate the

intestinal epithelial barrier damage. ZO-1 participated in maintaining the integrity of the intestinal epithelium via connecting other tight junctions (Occludin and Claudin-1) (Almousa, FranOis, Krol, & Jane, 2018). The mucus layers attached to the intestinal epithelial barrier were mainly composed of mucins secreted by goblet cells. Meanwhile, the mucins combined tight junctions to protect the intestinal barrier and resist the invasion of extrinsic substances together (Birchenough, Nystrom, Johansson, & Hansson, 2016). These results demonstrated that GLP-1.6 M significantly relieved LPS-induced intestinal barrier damage and enhanced the intestinal barrier function by up-regulating the expressions of MUC-2 and tight junctions (ZO-1, Occludin and Claudin-1).

4. Conclusions

In summary, three purified fractions were isolated from the degradation product 5-GLP from *G. lemaneiformis* polysaccharide with UV/H_2O_2 treatment. The purified fractions were mainly composed of galactose, glucose and xylose. GLP-1.6 M was a typical sulfated red alga polysaccharide with a conformation of curved chains, containing the linear backbone of β-(1 → 3)- and α-(1 → 4)-linked galactosyl residues and anhydro-galactose units. Furthermore, in the LPS-induced IEC-6 cells model, GLP-1.6 M significantly relieved intestinal barrier damage and enhanced the intestinal barrier function (Fig. 5). Our results indicated that GLP-1.6 M might exert stronger anti-inflammatory activity by down-regulating the expressions of iNOS, TLR-4 and pro-inflammatory cytokines (TNF-α, IL-6 and IL-1β) and up-regulating the expression of anti-inflammatory cytokine (IL-10), which might be involved in TLR-4/NF-κB pathway. Therefore, the purified polysaccharide from *G. lemaneiformis* could be a promising candidate for maintaining intestinal health in the food and pharmaceutical industries.

Declaration of Competing Interest

The authors declare that they have no known competing financial interests or personal relationships that could have appeared to influence the work reported in this paper.

Acknowledgements

This work was supported by the Guangzhou Science and Technology Program (201907010035); the National Natural Science Foundation of China (31972011), Excellent Youth Foundation of Guangdong Scientific Committee (No. 2021B1515020037), Program of Department of Natural Resources of Guangdong Province, the Natural Science Foundation of Guangdong Province (2019A1515011670), the 111 project (B17018) and the Fundamental Research Funds for the Central Universities (2019MS101).

Appendix A. Supplementary data

Supplementary data to this article can be found online at https://doi.org/10.1016/j.fochx.2021.100157.

References:

Adam, Drewnowski, S. E., & Specter. (2004). Poverty and obesity: The role of energy density and energy costs. *The American Journal of Clinical Nutrition, 79*(1), 6–16. https://doi.org/10.1093/ajcn/79.1.6

Almousa, A. A., FranOis, M., Krol, E. S., & Jane, A. (2018). Linoorbitides and enterolactone mitigate inflammation-induced oxidative stress and loss of intestinal epithelial barrier integrity. *International Immunopharmacology, 64*, 42–51. https://doi.org/10.1016/j.intimp.2018.08.012

Aquino, R. S., Landeira-Fernandez, A. M., Valente, A. P., Andrade, L. R., & Mourao, P. A. S. (2005). Occurrence of sulfated galactans in marine angiosperms: Evolutionary implications. *Glycobiology, 15*(1), 11–20. https://doi.org/10.1093/glycob/cwh138

Bilan, M. I., Vinogradova, E. V., Shashkov, A. S., & Usov, A. I. (2007). Structure of a highly pyruvylated galactan sulfate from the Pacific green alga *Codium yezoense* (*Bryopsidales, Chlorophyta*). *Carbohydrate Research, 342*(3–4), 586–596. https://doi.org/10.1016/j.carres.2006.11.008

Birchenough, G. M. H., Nystrom, E. E. L., Johansson, M. E. V., & Hansson, G. C. (2016). INNATE IMMUNITY A sentinel goblet cell guards the colonic crypt by triggering Nlrp6-dependent Muc2 secretion. *Science, 352*(6293), 1535–1542. https://doi.org/10.1126/science.aaf7419

Bo, Y. Y., Liang, L. D., Hua, Y. J., Zhao, Z., Yao, M. S., Shan, L. B., & Liang, C. Z. (2021). High-purity DNA extraction from animal tissue using picking in the TRIzol-based method. *Biotechniques, 70*(3), 186–190. https://doi.org/10.2144/btn-2020-0142

Chattopadhyay, K., Ghosh, T., Pujol, C. A., Carlucci, M. J., Damonte, E. B., & Ray, B. (2008). Polysaccharides from *Gracilaria corticata*: Sulfation, chemical characterization and anti-HSV activities. *International Journal of Biological Macromolecules, 43*(4), 346–351. https://doi.org/10.1016/j.ijbiomac.2008.07.009

Chen, C., You, L. J., Abbasi, A. M., Fu, X., & Liu, R. H. (2015). Optimization for ultrasound extraction of polysaccharides from mulberry fruits with antioxidant and hyperglycemic activity *in vitro*. *Carbohydrate Polymers, 130*, 122–132. https://doi.org/10.1016/j.carbpol.2015.05.003

Chen, D., Wu, X. Z., & Wen, Z. Y. (2008). Sulfated polysaccharides and immune response: Promoter or inhibitor? *Panminerva Medica, 50*(2), 177–183. https://pubmed.ncbi.nlm.nih.gov/18607341/.

Cheng, J. J., Chao, C. H., Chang, P. C., & Lu, M. K. (2016). Studies on anti-inflammatory activity of sulfated polysaccharides from cultivated *fungi Antrodia cinnamomea*. *Food Hydrocolloids, 53*, 37–45. https://doi.org/10.1016/j.foodhyd.2014.09.035

Du, B., Lin, C., Bian, Z., & Xu, B. (2015). An insight into anti-inflammatory effects of fungal beta-glucans. *Trends in Food Science and Technology, 41*(1), 49–59. https://doi.org/10.1016/j.tifs.2014.09.002

Farias, W. R. L., Valente, A. P., Pereira, M. S., & Mourao, P. A. S. (2000). Structure and anticoagulant activity of sulfated galactans - Isolation of a unique sulfated galactan from the red algae *Botryocladia occidentalis* and comparison of its anticoagulant action wtth that of sulfated galactans from *invertebrates*. *Journal of Biological Chemistry, 275*(38), 29299–29307. https://doi.org/10.1074/jbc.M002422200

Fitzgerald, K. A., & Kagan, J. C. (2020). Toll-like Receptors and the Control of Immunity. *Cell, 180*(6), 1044–1066. https://doi.org/10.1016/j.cell.2020.02.041

Gandhi, G. R., Vasconcelos, A. B. S., Haran, G. H., Calisto, V. K.da. S., Jothi, G., Quintans, J.de. S. S., … Gurgel, R. Q. (2020). Essential oils and its bioactive compounds modulating cytokines: A systematic review on anti-asthmatic and immunomodulatory properties. *Phytomedicine, 73*, 152854. https://doi.org/10.1016/j.phymed.2019.152854

Gen, L., Mingming, S., Jun, W., & Ge.. (2015). Identification and biochemical characterization of a novel endo-type β-agarase AgaW from *Cohnella* sp. strain LGH. *Applied Microbiology and Biotechnology, 99*(23), 10019–10029. https://doi.org/10.1007/s00253-015-6869-6

Gong, Y., Ma, Y., Cheung, P.-K., You, L., Liao, L., Pedisić, S., & Kulikouskaya, V. (2021). Structural characteristics and anti-inflammatory activity of UV/H_2O_2-treated algal sulfated polysaccharide from *Gracilaria lemaneiformis*. *Food and Chemical Toxicology, 152*, 112157. https://doi.org/10.1016/j.fct.2021.112157

Graham, D. B., & Xavier, R. J. (2020). Pathway paradigms revealed from the genetics of inflammatory bowel disease. *Nature, 578*(7796), 527–539. https://doi.org/10.1038/s41586-020-2025-2

Jiao, G., Yu, G., Zhang, J., & Ewart, H. S. (2011). Chemical structures and bioactivities of sulfated polysaccharides from marine algae. *Marine Drugs, 9*(2), 196–223. https://doi.org/10.3390/md9020196

Khan, B. M., Qiu, H. M., Xu, S. Y., Liu, Y., & Cheong, K. L. (2020). Physicochemical characterization and antioxidant activity of sulphated polysaccharides derived from *Porphyra haitanensis*. *International Journal of Biological Macromolecules, 145*, 1155–1161. https://doi.org/10.1016/j.ijbiomac.2019.10.040

Krol, Z., Malik, M., Marycz, K., & Jarmoluk, A. (2016). Physicochemical properties of biopolymer hydrogels treated by direct electric current. *Polymers, 8*(7), 248. https://doi.org/10.3390/polym8070248

Lahaye, M., Revol, J. F., Rochas, C., McLachlan, J., & Yaphe, W. (1988). The chemical structure of *Gracilaria crassissima*. *Botanica Marina, 37*, 491–495. https://doi.org/10.1515/botm.1988.31.6.491

Lee, K. P., Sudjarwo, G. W., Kim, J.-S., Dirgantara, S., Maeng, W. J., & Hong, H. (2014). The anti-inflammatory effect of *Indonesian Areca* catechu leaf extract *in vitro* and *in vivo*. *Nutrition Research and Practice, 8*(3), 267–271. https://doi.org/10.4162/nrp.2014.8.3.267

Li, C., Duan, S., Li, Y., Pan, X., & Han, L. (2021). Polysaccharides in natural products that repair the damage to intestinal mucosa caused by cyclophosphamide and their mechanisms: A review. *Carbohydrate Polymers, 261*, 117876. https://doi.org/10.1016/j.carbpol.2021.117876

Li, J., Zhang, L., Wu, T., Li, Y., Zhou, X., & Ruan, Z. (2021). Indole-3-propionic acid improved the intestinal barrier by enhancing epithelial barrier and mucus barrier. *Journal of Agricultural and Food Chemistry, 69*(5), 1487–1495. https://doi.org/10.1021/acs.jafc.0c0520510.1021/acs.jafc.0c05205.s001

Li, X., Huang, S., Chen, X., Xu, Q., Ma, Y., You, L., … Piao, J. (2020). Structural characteristic of a sulfated polysaccharide from *Gracilaria Lemaneiformis* and its lipid metabolism regulation effect. *Food and Function, 11*(12), 10876–10885. https://doi.org/10.1039/D0FO02575E

Liu, Q., Yu, Z., Tian, F., Zhao, J., Zhang, H., Zhai, Q., & Chen, W. (2020). Surface components and metabolites of probiotics for regulation of intestinal epithelial barrier. *Microbial Cell Factories, 19*(1), 23. https://doi.org/10.1186/s12934-020-1289-4

Mueller, M., Hobiger, S., & Jungbauer, A. (2010). Anti-inflammatory activity of extracts from fruits, herbs and spices. *Food Chemistry, 122*(4), 987–996. https://doi.org/10.1016/j.foodchem.2010.03.041

Murano, E., Toffanin, R., Zanetti, F., Knutsen, S. H., Paoletti, S., & Rizzo, R. (1992). Chemical and macromolecular characterisation of agar polymers from *Gracilaria dura* (C. Agardh) J. Agardh (*Gracilariaceae, Rhodophyta*). *Carbohydrate Polymers, 18* (3), 171–178. https://doi.org/10.1016/0144-8617(92)90061-T

Niu, X., Shang, H., Chen, S., Chen, R., Huang, J., Miao, Y., … Zhu, R. (2021). Effects of *Pinus massoniana* pollen polysaccharides on intestinal microenvironment and colitis in mice. *Food and Function, 12*(1), 252–266. https://doi.org/10.1039/D0FO02190C

Okumura, R., & Takeda, K. (2018). Maintenance of intestinal homeostasis by mucosal barriers. *Inflammation and Regeneration, 38*(1). https://doi.org/10.1186/s41232-018-0063-z

Qi, H. M., Zhang, Q. B., Zhao, T. T., Chen, R., Zhang, H., Niu, X. Z., & Li, Z. (2005). Antioxidant activity of different sulfate content derivatives of polysaccharide extracted from Ulva pertusa (Chlorophyta) *in vitro*. *International Journal of Biological Macromolecules, 37*(4), 195–199. https://doi.org/10.1016/j.ijbiomac.2005.10.008

Sen, M., & Erboz, R. N. (2010). Determination of critical gelation conditions of κ-carrageenan by viscosimetric and FT-IR analyses. *Food Research International, 43* (5), 1361–1364. https://doi.org/10.1016/j.foodres.2010.03.021

Singh, S., Bhatia, R., Singh, A., Singh, P., Kaur, R., Khare, P., … Kondepudi, K. K. (2018). Probiotic attributes and prevention of LPS-induced pro-inflammatory stress in RAW264.7 macrophages and human intestinal epithelial cell line (Caco-2) by newly isolated Weissella cibaria strains. *Food and Function, 9*(2), 1254–1264. https://doi.org/10.1039/C7FO00469A

Veeraperumal, S., Qiu, H.-M., Zeng, S.-S., Yao, W.-Z., Wang, B.-P., Liu, Y., & Cheong, K.-L. (2020). Polysaccharides from *Gracilaria lemaneiformis* promote the HaCaT keratinocytes wound healing by polarised and directional cell migration. *Carbohydrate Polymers, 241*, 116310. https://doi.org/10.1016/j.carbpol.2020.116310

Vidya, M. K., Kumar, V. G., Sejian, V., Bagath, M., Krishnan, G., & Bhatta, R. (2018). Toll-like receptors: Significance, ligands, signaling pathways, and functions in mammals. *International Reviews of Immunology, 37*(1), 20–36. https://doi.org/10.1080/08830185.2017.1380200

Volery, P., Besson, R., & Schaffer-Lequart, C. (2004). Characterization of commercial carrageenans by Fourier transform infrared spectroscopy using single-reflection attenuated total reflection. *Journal of Agricultural and Food Chemistry, 52*(25), 7457–7463. https://doi.org/10.1021/jf040229o

Wilms, H., Sievers, J., Rickert, U., Rostami-Yazdi, M., Mrowietz, U., & Lucius, R. (2010). Dimethylfumarate inhibits microglial and astrocytic inflammation by suppressing the synthesis of nitric oxide, IL-1 beta, TNF-alpha and IL-6 in an in-vitro model of brain inflammation. *Journal of Neuroinflammation, 7*. https://doi.org/10.1186/1742-2094-7-30

Xu, X., Chang, Y., Xue, C., Wang, J., & Shen, J. (2018). Gastric protective activities of sea cucumber fucoidans with different molecular weight and chain conformations: A structure-activity relationship investigation. *Journal of Agricultural and Food Chemistry, 66*(32), 8615–8622. https://doi.org/10.1021/acs.jafc.8b0149710.1021/acs.jafc.8b01497.s001

You, L., Gong, Y., Li, L., Hu, X., Brennan, C., & Kulikouskaya, V. (2020). Beneficial effects of three brown seaweed polysaccharides on gut microbiota and their structural characteristics: An overview. *International Journal of Food Science and Technology, 55* (3), 1199–1206. https://doi.org/10.1111/ijfs.v55.310.1111/ijfs.14408

Yu, Z., Liu, L., Xu, Y., Wang, L., Teng, X., Li, X., & Dai, J. (2015). Characterization and biological activities of a novel polysaccharide isolated from raspberry (*Rubus idaeus L.*) fruits. *Carbohydrate Polymers, 132*, 180–186. https://doi.org/10.1016/j.carbpol.2015.06.068

Zhao, L., Li, M., Sun, K., Su, S., Geng, T., & Sun, H. (2020). Hippophae rhamnoides polysaccharides protect IPEC-J2 cells from LPS-induced inflammation, apoptosis and barrier dysfunction *in vitro* via inhibiting TLR4/NF-kappaB signaling pathway. *International Journal of Biological Macromolecules, 155*, 1202–1215. https://doi.org/10.1016/j.ijbiomac.2019.11.088

Zhuang, S., Zhong, J., Zhou, Q., Zhong, Y., Liu, P., & Liu, Z. (2019). Rhein protects against barrier disruption and inhibits inflammation in intestinal epithelial cells. *International Immunopharmacology, 71*, 321–327. https://doi.org/10.1016/j.intimp.2019.03.030